

## Two-Channel Kondo Effect in a Modified Single Electron Transistor

Yuval Oreg<sup>1</sup> and David Goldhaber-Gordon<sup>2</sup>

<sup>1</sup>*Department of Condensed Matter Physics, Weizmann Institute of Science, Rehovot 76100, Israel*

<sup>2</sup>*Geballe Laboratory for Advanced Materials and Department of Physics, Stanford University, Stanford, California 94305*

(Received 13 March 2002; published 2 April 2003)

We suggest a simple system of two electron droplets which should display two-channel Kondo behavior at experimentally accessible temperatures. Stabilization of the two-channel Kondo fixed point requires fine control of the electrochemical potential in each droplet, which can be achieved by adjusting voltages on nearby gate electrodes. We study the conditions for obtaining this type of two-channel Kondo behavior, discuss the experimentally observable consequences, and explore the generalization to the multichannel Kondo case.

DOI: 10.1103/PhysRevLett.90.136602

PACS numbers: 72.15.Qm, 68.65.Hb, 71.27.+a

The single-channel Kondo (ICK) effect has been studied for decades in metals with magnetic impurities [1]. The same phenomenon has recently been observed in the novel context of semiconductor nanostructures containing no magnetic impurities: Here, an electron droplet with a degenerate ground state assumes the role of a magnetic impurity, and nearby electron reservoirs act as the surrounding normal metal [2–7]. These semiconductor systems are extremely flexible. The electron droplet's shape and size are determined by lithographic patterning, and its occupancy, energy levels, and coupling to external reservoirs can be precisely measured, and even tuned *in situ* using gate voltages. This unique tunability has enabled the first precision measurements of Kondo temperature as a function of system parameters, yielding an excellent match to theory [4,8]. Experiments on semiconductor nanostructures have also accessed new regimes, notably the low-temperature unitary limit [5], Kondo effect out of equilibrium [9], and the single mixed-valence impurity [4]. These experiments have even introduced exotic varieties of Kondo effect never seen in bulk studies, such as magnetic field-induced Kondo [10,11] and two-impurity Kondo [12]. As with conventional ICK, each of these systems displays an interesting many-body resonance. However, at very low temperature  $T$ , we can describe each system simply as a Fermi liquid superimposed with a resonance [13]; i.e., there is no non-Fermi liquid ground state.

Studying the two-channel Kondo (2CK) effect [14–18] in semiconductor nanostructures could be even more intriguing. In 2CK, a twofold degenerate system such as a local spin is antiferromagnetically coupled to not one, but two independent electron reservoirs. Since the reservoirs do not communicate, each attempts to screen the local spin, resulting in overall overscreening. Unlike ICK, this system exhibits fascinating low-energy non-Fermi-liquid behavior [19,20]. Yet there have been no conclusive experimental observations of 2CK [14,16,21]. Indeed, in contrast to single-channel Kondo, the 2CK effect is not likely to occur in ordinary metals with magnetic impurities, due to intrinsic channel anisotropy [22]. Ralph re-

ported observation of 2CK, with local near-degeneracies associated with atomic tunneling in a disordered metal rather than the traditional spin. The observed behavior is striking, but its physical origin has remained controversial [16,21].

In this Letter, we argue that a simple configuration of two electron droplets (see Fig. 1) attached to conducting leads can exhibit 2CK correlations [19,20], retaining non-Fermi-liquid (NFL) behavior at low temperature. The relevant fixed point is stabilized at low temperature by fine-tuning the voltage on just one gate electrode. Near a 2CK fixed point, quantities such as specific heat, entropy, and spin susceptibility [20] behave differently than they would in a Fermi liquid. The conductance through our model system should exhibit an anomalous power-law dependence on temperature, deviating from its  $T = 0$  value as  $\sqrt{T}$  [20] rather than  $T^2$ . The simplicity of the

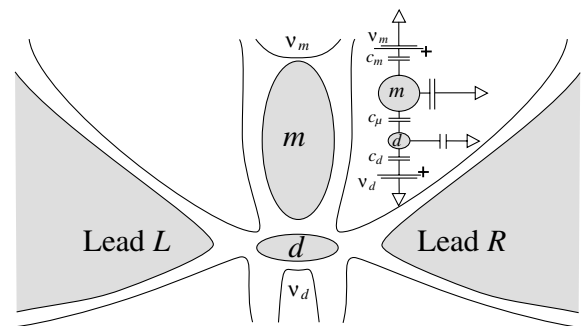


FIG. 1. A proposed realization of the two-channel Kondo (2CK) model. Two noninteracting leads ( $L$  and  $R$ ) and a large dot  $m$  are attached to a single-level small dot  $d$ . If dot  $d$  is occupied by a single electron, it can flip its spin by virtually hopping the electron onto either dot  $m$  or the leads, and then returning an electron with opposite spin to dot  $d$ . Dot  $m$  and the leads thus serve as the two distinct screening channels required to produce the 2CK effect. Crucially, when  $kT$  is smaller than the charging energy of dot  $m$ , Coulomb blockade blocks transfer of electrons between the leads and dot  $m$ . Fine-tuning of the voltage  $V_m$  (and/or  $V_d$ ) can equalize the coupling to the two channels, stabilizing the 2CK fixed point.

structure and the ability to tune system parameters offer hope for detailed study of the NFL realm, including nonthermodynamic quantities such as transmission phase [23], noise [24], pumping [25], and tunneling density of states.

In our model, a small central electron droplet (denoted by  $d$ ) hosts a single level of energy  $\varepsilon_{ds}$ , which can be empty, or occupied by electrons of either or both spin directions  $s = \uparrow, \downarrow$ . Henceforth we refer to this droplet as *small dot  $d$* . The spin of the (singly occupied) small dot  $d$  serves as the local degeneracy needed for 2CK. Connected to small dot  $d$  by tunneling are two conducting leads, plus an additional, much larger dot. In the large dot, we neglect the discreteness of single-particle energy levels, while retaining a finite Coulomb energy. Thus, this dot behaves as a ‘‘Coulomb-interacting lead’’; we refer to it as *large dot  $m$* .

For a fixed number of electrons:  $n_m$  on dot  $m$  and  $n_d$  on dot  $d$ , the electrostatic energy  $E_{n_d}^{n_m} \equiv E_{n_d}^{n_m}(\mathcal{V}_m, \mathcal{V}_d)$  is

$$E_{n_d}^{n_m} = U(n_d - \mathcal{N}_d)^2 + u_m(n_d + \alpha n_m - \mathcal{N})^2, \quad (1)$$

where  $U \equiv e^2/(2\tilde{C}_d) \gg u_m \equiv e^2/(2\tilde{C}_m - c_\mu^2/\tilde{C}_d)$ ,  $|e|\mathcal{N}_d \equiv c_d\mathcal{V}_d$ ,  $|e|\mathcal{N} \equiv c_m\mathcal{V}_m + c_d c_\mu/\tilde{C}_m\mathcal{V}_d$ , and  $\alpha \equiv c_\mu/\tilde{C}_d \lesssim 1$ . Here,  $\tilde{C}_{m(d)}$  is the *total* capacitance of dot  $m(d)$ . See Fig. 1 for definitions of the other capacitances. Note that the parameter  $\mathcal{N}_d$  controls the number of electrons on the small dot while  $\mathcal{N}$  controls the total number of electrons on both dots combined. Since dot  $m$  is large, we may assume that  $\tilde{C}_m$  is much larger than all other capacitances.

To write down the full Hamiltonian  $H$  of the model system, it is useful to perform a transformation on the operators  $L_{ks}$  and  $R_{ks}$  for electrons in leads  $L$  and  $R$ , respectively [26]. We define  $\psi_{ks} = \cos\theta L_{ks} + \sin\theta R_{ks}$ ,  $\phi_{ks} = \cos\theta R_{ks} - \sin\theta L_{ks}$ ,  $\tan\theta = V_R/V_L$ , and  $V_\psi = \sqrt{|V_L|^2 + |V_R|^2}$ . Without loss of generality, we take the coupling constants  $V_i$ ,  $i = L, R, m$ , to be real. With these definitions, the new effective lead  $\psi$  couples to the small dot  $d$ , but the effective lead  $\phi$  does not couple:

$$H = \sum_{i=\phi,\psi,m;ks} \varepsilon_{iks} i_{ks}^\dagger i_{ks} + \sum_s \varepsilon_{ds} d_s^\dagger d_s + E_{n_d}^{n_m} + V_m \sum_{ks} m_{ks}^\dagger d_s + V_\psi \sum_{ks} \psi_{ks}^\dagger d_s + \text{H.c.}, \quad (2)$$

To obtain a 2CK fixed point, we assume that  $\mathcal{V}_d$  is tuned to make the average occupancy of the small dot  $n_d = 1$ , creating a local spin  $\frac{1}{2}$ . We further assume that  $D, U \gg u_m$ , with  $D$  a cutoff of the order of the Fermi energy [27]. With decreasing temperature, the system evolves through several stages. Formally, we integrate out the fast variables progressively in the renormalization group (RG) sense. Details of this calculation will be published elsewhere.

For  $kT > U$ , charge fluctuations on both the small and large dots are possible. Haldane showed [8] that in this regime only the level energy  $\varepsilon_d$  is renormalized, while

the couplings to the leads remain the same. For  $kT \lesssim U$ , we may perform the Schrieffer-Wolff transformation. In this transformation charge fluctuations on the small dot are eliminated, and the effect of virtual electron hopping is simply to flip the spin on the small dot. Our Anderson-like Hamiltonian is mapped onto a ICK Hamiltonian. In the present case, we have four possible spin flip events. Two are diagonal processes in which an electron hops onto dot  $d$  from lead  $\psi$  (large dot  $m$ ) and then an electron with opposite spin hops off to the same lead  $\psi$  (large dot  $m$ ). Two are off-diagonal processes in which an electron hops onto dot  $d$  from lead  $\psi$  (large dot  $m$ ) and then an electron with opposite spin hops off to large dot  $m$  (lead  $\psi$ ). (Four ‘‘hole’’ processes, in which an electron first hops *from* the dot to lead  $\psi$  or large dot  $m$ , are also possible). As  $T$  decreases further, so long as  $kT > u_m$ , charge fluctuations on large dot  $m$  are allowed and the system flows according to the single-channel Kondo RG laws [8]. However, for  $kT < u_m$ , charge fluctuations on the large dot are not possible and off-diagonal hopping is suppressed. Diagonal spin flip events remain possible. In this regime, we obtain the standard two-channel Kondo model [20], with an additional free channel  $\phi$  which decouples from the rest of the system [see also Eq. (6)]. The diagonal exchange coupling constants (at scale  $U$ ) are

$$\begin{aligned} \tilde{J}_{mm}(\mathcal{V}_m, \mathcal{V}_d) &\equiv \Gamma_m \left[ \frac{1}{E_0^1 - E_1^0} + \frac{1}{E_2^{-1} - E_1^0} \right]; \\ \tilde{J}_{\psi\psi}(\mathcal{V}_m, \mathcal{V}_d) &\equiv \Gamma_\psi \left[ \frac{1}{E_2^0 - E_1^0} + \frac{1}{E_0^0 - E_1^0} \right]. \end{aligned} \quad (3)$$

Here  $\Gamma_{m(\psi)} = |V_{m(\psi)}|^2 \nu_{m(\psi)}$  is the rate of tunneling between dot  $d$  and dot  $m$  (effective lead  $\psi$ ); and  $E_{n_d}^{n_m}$  are defined in Eq. (1). To obtain a 2CK fixed point, we tune  $\mathcal{V}_m$  and  $\mathcal{V}_d$  to make  $\tilde{J}_{mm}$ , the antiferromagnetic coupling of dot  $d$  to dot  $m$ , equal to  $\tilde{J}_{\psi\psi}$ , the antiferromagnetic coupling of dot  $d$  to the leads. Equation (3) and the ratio  $\gamma \equiv \Gamma_m/\Gamma_\psi$  define a curve in the  $\mathcal{V}_m, \mathcal{V}_d$  plane. In Fig. 2, we show these ‘‘2CK lines’’ for two different values of  $\gamma$ , both of order 1. On these lines, 2CK physics should be realized at low  $T$ . We did not consider in Fig. 2 the renormalization of the parameters at scales below  $U$ , which may modify the detailed shape of the curves.

The 2CK fixed point can be reached experimentally by a three-step procedure: First, fix  $\mathcal{V}_d$  to give one electron (or an odd number of electrons) in the small dot. Second, tune  $\gamma$  to roughly 1 by adjusting the individual tunneling rates. No great precision is required in this step. Finally, fine-tune  $\mathcal{V}_m$  so that  $\tilde{J}_{mm}(\mathcal{V}_m, \mathcal{V}_d) = \tilde{J}_{\psi\psi}(\mathcal{V}_m, \mathcal{V}_d)$ . In Fig. 2, this corresponds to tuning  $\mathcal{V}_m$  until we hit a 2CK line for our given value of  $\gamma$ .

The current  $I$  between the left and right leads can be measured as a function of  $T$ , and as a function of  $\mathcal{V}_{LR}$ , the bias applied between leads  $L$  and  $R$  (see Fig. 1). Drawing on the extensive literature of 2CK physics [14], we can predict the qualitative behavior of the  $I$ - $\mathcal{V}_{LR}$  curve through the dot, for different values of the gate

voltages  $\mathcal{V}_m, \mathcal{V}_d$  that scan the hexagon of Fig. 2. On the 2CK lines (see Fig. 2) in the unitary limit— $T, \mathcal{V}_{RL} \ll$  Kondo temperature  $T_K$ —the differential conductance  $G(T, \mathcal{V}_{LR}) \equiv dI/d\mathcal{V}_{LR}$  should approach its limiting value  $G(0, 0)$  as

$$2\text{CK: } G(0, 0) - G(T, \mathcal{V}_{LR}) \propto \sqrt{\max(\mathcal{V}_{LR}, kT)}. \quad (4a)$$

In the symmetric case  $V_L = V_R$ , we get  $G(0, 0) = G_K \equiv e^2/h$ , half the maximal value of  $G(0, 0)$  in the 1CK effect [5,7]. In the part of the hexagon where  $\tilde{J}_{mm} > \tilde{J}_{\psi\psi}$  (shaded, for  $\gamma = 1.08$ ), at low  $T$  the electrons in dot  $m$  screen the spin of dot  $d$ , while the leads are decoupled. In the RG sense  $\tilde{J}_{\psi\psi}$  flows to zero, so that dot  $m$  “wins” over the leads and forms a 1CK state with dot  $d$ . In this case,  $dI/d\mathcal{V}_{LR}$  is small and given by

$$\text{large dot wins: } G(T, \mathcal{V}_{LR}) \propto [\max(\mathcal{V}_{LR}, kT)]^2. \quad (4b)$$

In contrast, in the unshaded part of the hexagon in Fig. 2, where  $\tilde{J}_{mm} < \tilde{J}_{\psi\psi}$ , dot  $m$  decouples from dot  $d$  at low  $T$ , leaving the leads to form a 1CK resonance with dot  $d$  and

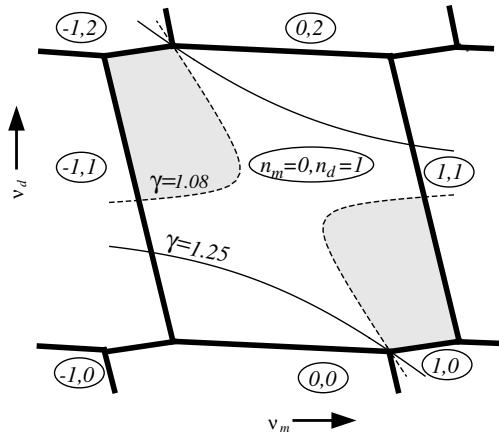


FIG. 2. The number of electrons on dots  $m$  and  $d$  are functions of the gate voltages  $\mathcal{V}_m$  and  $\mathcal{V}_d$ . Within the central hexagon, dot  $d$  is singly occupied, a prerequisite for observation of the Kondo effect. Curves superimposed on this hexagon (“2CK lines”) map where in the  $\mathcal{V}_m, \mathcal{V}_d$  plane the two-channel Kondo (2CK) effect is realized for two different values of the coupling ratio  $\gamma \equiv \Gamma_m/\Gamma_\psi$ —each value gives rise to a pair of disjoint curves. As illustrated for  $\gamma = 1.08$  (dashed lines), these two curves divide the hexagon into three regions with distinct low-temperature fixed points. On the curves, the 2CK effect is realized and the deviation of the interlead differential conductance from its  $T \rightarrow 0, \mathcal{V}_{LR} \rightarrow 0$  limit  $G(0, 0)$  is  $\propto \sqrt{\max(T, \mathcal{V}_{LR})}$  [Eq. (4a)]. In the shaded regions at the top left and bottom right, dot  $m$  “wins,” forming an exclusive 1CK resonance with dot  $d$ , and driving  $G(T, \mathcal{V}_{LR})$  close to zero [Eq. (4b)]. By contrast, in the large unshaded region, leads  $L$  and  $R$  “win” giving rise to familiar Fermi-liquid behavior  $G(0, 0) - G(T, \mathcal{V}_{LR}) \propto [\max(T, \mathcal{V}_{LR})]^2$  [Eq. (4c)]. With increasing  $\gamma$ , the regions where dot  $m$  wins grow and merge, while the region where the leads win shrinks and splits.

$$\text{leads win: } G(0, 0) - G(T, \mathcal{V}_{LR}) \propto [\max(\mathcal{V}_{LR}, kT)]^2, \quad (4c)$$

where  $G(0, 0) = 2G_K$  for  $V_L = V_R$ .

At sufficiently low temperature, the finite level spacing  $\Delta_m$  in dot  $m$  will cut off the RG flow of the coupling constants [28]. We cannot make  $\Delta_m$  infinitesimal as we must retain a finite Coulomb blockade energy [29]  $u_m > kT$ . However, the ratio between charging energy and level spacing can be made large, allowing 2CK behavior to be observed over an order of magnitude in temperature before the system finally flows to the 1CK fixed point.

The above discussion can be generalized to include  $M - 1$  large dots, resulting in an  $M$ -channel Kondo (MCK) model, which may be possible (though challenging) to realize experimentally for  $M > 2$ .

To describe this system, we use the model

$$H = \sum_{aks} \varepsilon_{aks} a_{ks}^\dagger a_{ks} + \sum_a u_a (n_a - \mathcal{N}_a)^2 + \sum_s \varepsilon_d d_s^\dagger d_s + U n_d n_{d\downarrow} + \sum_{ks} V_{ak}^* a_{ks}^\dagger d_s + \text{H.c.} \quad (5)$$

Here  $a_{ks}$  is the annihilation operator of an electron in state  $k$ , with spin  $s$  and energy  $\varepsilon_{aks}$  on large dot  $a$ .  $a = 1, \dots, M$ ,  $n_a = \sum_{ks} a_{ks}^\dagger a_{ks}$ , and the parameter  $\mathcal{N}_a$  sets dot  $a$  equilibrium occupancy.

The physical role of the  $u_a$  terms is clear: At low temperatures they forbid processes in which charge is ultimately transferred from one large dot to another. Spin flip events—e.g., when an electron hops onto the small dot and then an electron with opposite spin hops off the small dot to the same large dot—remain possible and under appropriate conditions lead to a MCK fixed point.

After integrating out energies larger than  $U$  [8], we perform the Schrieffer-Wolff transformation [30] and find that the second line of Eq. (5) is transformed to

$$\sum_{ab,kq} J_{ab}^{kq} [S_{ab}^+ s_{ab}^{-kq} + S_{ab}^- s_{ab}^{+kq} + 2S_{ab}^z s_{ab}^{zkq}], \quad (6)$$

$S_{ab}^\pm = d_{(l)}^\dagger d_{(l)}$ ,  $2S_{ab}^z = d_{(l)}^\dagger d_{(l)} - d_{(l)}^\dagger d_{(l)}$ ,  $s_{ab}^{\pm kq} = a_{k(l)}^\dagger b_{q(l)}$ , and  $2s_{ab}^{zkq} = \frac{1}{2} a_{k(l)}^\dagger b_{q(l)} - a_{k(l)}^\dagger b_{q(l)}$ . With  $V_{aq} = V_{bk} \equiv V$ , and assuming that  $\varepsilon_{a(b)qs} \approx \varepsilon_{a(b)F}$ , where  $\varepsilon_{a(b)F}$  is the last empty (occupied) level in dot  $a$  ( $b$ ), we find

$$J_{ab}^{kq} = J_{ab} = |V|^2 \frac{U + u_b^- + u_a^+}{[U + \varepsilon_d + u_b^-][u_a^+ - \varepsilon_d]}, \quad (7)$$

where  $u_p^\pm = u_p [1 \pm 2(n_p - \mathcal{N}_p)] \pm \varepsilon_{pF}$ ,  $p = a, b$ . For  $-1/2 < \mathcal{N}_p - n_p + (\mu - \varepsilon_{pF})/(2u_p) < 1/2$ , there are  $n_p$  electrons in dot  $p$ , where  $\mu$  is the electrochemical potential of a reference reservoir. Particle-hole symmetry may be absent in the large dots, so in general  $J_{ab} \neq J_{ba}$ .

At  $kT > \max\{u_{ab}\}$ , the system evolves according to the 1CK RG flow, where  $u_{ab} = (u_a^+ + u_b^-)(1 - \delta_{ab})$ . At  $kT < \min\{u_{ab}\}$ ,  $a \neq b$ , the off-diagonal processes describing transfer of an electron from dot  $b$  to dot  $a$  are exponentially suppressed as  $J_{ab} = J_{ab}^0 e^{u_{ab}/(4kT)}$ . Notice that  $u_{aa} = 0$ , since the charge on dot  $a$  is not changed

when an electron hops from dot  $a$  onto dot  $d$  and then back to the same dot  $a$ . At  $kT < \min\{u_{ab}\}$ , only the diagonal terms of  $J_{ab}$  do not flow to zero. Assuming that we are not at a degeneracy point where  $u_{ab} = 0$ , an easy condition to avoid, the RG equations are identical to the MCK RG equations [22]. As in the case of classic MCK, our NFL fixed point is unstable to channel anisotropy. If one of the coupling constants is larger than the others, the corresponding channel alone screens the local spin and forms a Kondo resonance while the other channels are decoupled from the local spin. In our model, we can tune all the  $\mathcal{N}_a$  to achieve  $J_{aa} = J$  for all  $a$ .

Gate voltages capacitively control the energy of the last occupied level in each large dot, so excitations in each large dot will be around a different Fermi energy. This does not modify the RG equations, but does affect certain physical properties such as the small dot density of states at finite energies. A similar situation occurs in the discussion of 2CK in a dot out of equilibrium [15,18].

In conclusion, if a small dot is coupled to two (or more) electron reservoirs, the Coulomb blockade can suppress interreservoir charge transfer at low temperatures. Electrostatic gates provide the tunability needed to stabilize a 2CK fixed point, resulting in observable NFL behavior. Softer suppressions of interreservoir tunneling could also work in place of Coulomb blockade. For example, the reservoirs could be conductors with large impedance [31], one-dimensional Luttinger liquids [32], or conductors with strongly interacting charge carriers. Finally, while the channel asymmetry parameter is relevant in the RG sense, for realistically well-matched channel couplings we expect that the system will remain near the 2CK fixed point, and will show NFL behavior, over a wide range of temperatures.

It is our pleasure to acknowledge useful discussions with Natan Andrei, Michel Devoret, Leonid Glazman, Gabi Kotliar, Leo Kouwenhoven, Yigal Meir, Ron Potok, Arcadi Shehter, Alex Silva, Ned Wingreen, and especially Avi Schiller. This work was supported by DIP Grant No. c-7.1, by the Minerva fund, and by Stanford University.

- 
- [1] A.C. Hewson, *The Kondo Problem to Heavy Fermions* (Cambridge University Press, Cambridge, England, 1993).
- [2] D. Goldhaber-Gordon, H. Shtrikman, D. Mahalu, D. Abusch-Magder, U. Meirav, and M.A. Kastner, *Nature* (London) **391**, 156 (1998).
- [3] S.M. Cronenwett, T.H. Oosterkamp, and L.P. Kouwenhoven, *Science* **281**, 540 (1998).
- [4] D. Goldhaber-Gordon, J. Göres, M.A. Kastner, H. Shtrikman, D. Mahalu, and U. Meirav, *Phys. Rev. Lett.* **81**, 5225 (1998).
- [5] W.G. van der Wiel *et al.*, *Science* **289**, 2105 (2000).
- [6] J. Nygard, D.H. Cobden, and P.E. Lindelof, *Nature* (London) **408**, 342 (2000).

- [7] W. Liang, M. Bockrath, and H. Park, *Phys. Rev. Lett.* **88**, 126801 (2002).
- [8] F.D.M. Haldane, *Phys. Rev. Lett.* **40**, 416 (1978).
- [9] S. De Franceschi *et al.*, cond-mat/0203146.
- [10] S. Sasaki *et al.*, *Nature* (London) **405**, 764 (2000).
- [11] M. Pustilnik, Y. Avishai, and K. Kikoin, *Phys. Rev. Lett.* **84**, 1756 (2000); M. Pustilnik and L.I. Glazman, *Phys. Rev. B* **64**, 045328 (2001).
- [12] H. Jeong, A.M. Chang, and M.R. Melloch, *Science* **293**, 2221 (2001).
- [13] P. Nozières, *J. Low Temp. Phys.* **17**, 31 (1974).
- [14] D. Cox and A. Zawadowski, *Adv. Phys.* **47**, 599 (1998).
- [15] We emphasize that our proposal differs from other suggested experimental realizations of the 2CK effect [16,17], in that our local degeneracy comes from spin rather than charge or some other two-level system. Our mapping differs from that of [17] in several essential ways: We consider a system with fixed electron number in what would otherwise be a Coulomb valley, not a charge degeneracy point; our Kondo temperature is set by the charging energy of a small dot; and we do not require single-mode coupling between the dot and leads. Our 2CK effect is realized at equilibrium, avoiding decoherence and suppression of 2CK by voltage-driven current [18].
- [16] D.C. Ralph and R.A. Buhrman, *Phys. Rev. Lett.* **69**, 2118 (1992); *Phys. Rev. B* **51**, 3554 (1995); D.C. Ralph *et al.* *Phys. Rev. Lett.* **72**, 1064 (1994).
- [17] K.A. Matveev, *Phys. Rev. B* **51**, 1743 (1995).
- [18] A. Rosch, J. Kroha, and P. Wölfle, *Phys. Rev. Lett.* **87**, 156802 (2001).
- [19] N. Andrei and C. Destri, *Phys. Rev. Lett.* **52**, 364 (1984); A.M. Tvelick and P.B. Wiegmann, *Z. Phys. B* **54**, 201 (1984).
- [20] I. Affleck and A.W.W. Ludwig, *Phys. Rev. B* **48**, 7297 (1993).
- [21] N.S. Wingreen, B.L. Altshuler, and Y. Meir, *Phys. Rev. Lett.* **75**, 769 (1995); see also D.C. Ralph *et al.*, *ibid.*, **75**, 770 (1995); N.S. Wingreen *et al.*, *ibid.* **81**, 4280(E) (1998).
- [22] P. Nozières and A. Blandin, *J. Phys. (Paris)* **41**, 193 (1980).
- [23] U. Gerland *et al.*, *Phys. Rev. Lett.* **84**, 3710 (2000); Y. Ji *et al.*, *Science* **290**, 779 (2000).
- [24] R. de Picciotto *et al.*, *Nature* (London) **389**, 162 (1997).
- [25] M. Switkes *et al.*, *Science* **283**, 1905 (1999).
- [26] L.I. Glazman and M.E. Raikh, *Pis'ma Zh. Eksp. Teor. Fiz.* **47**, 378 (1988) [*JETP Lett.* **47**, 452 (1988)].
- [27] In semiconductor structures, generally  $D > U$ . We will assume this here, but relaxing this assumption has no significant impact on our conclusions.
- [28] W.B. Thimm, J. Kroha, and J. von Delft, *Phys. Rev. Lett.* **82**, 2143 (1999).
- [29] Our Kondo temperature is set by parameters of the small dot. For a small (large) dot of diameter 100 nm ( $2 \mu\text{m}$ ) in a GaAs/AlGaAs heterostructure, it is possible to achieve  $u_m \sim 3 \text{ K} > T_K \sim 1 \text{ K} \gg \Delta_m \sim 50 \text{ mK}$ .
- [30] J.R. Schrieffer and P.A. Wolff, *Phys. Rev.* **149**, 491 (1966).
- [31] M.H. Devoret *et al.*, *Phys. Rev. Lett.* **64**, 1824 (1990).
- [32] M. Fabrizio and A.O. Gogolin, *Phys. Rev. B* **51**, 17827 (1995).